Conformational Study of Solid Polypeptides by ^{1}H Combined Rotation and Multiple Pulse Spectroscopy NMR. 2. Amide Proton Chemical Shift

Hideaki Kimura,† Takuo Ozaki,† Hisashi Sugisawa,‡ Kenzo Deguchi,‡ and Akira Shoji*,†

Department of Biological Sciences, Faculty of Engineering, Gunma University, 1-5-1, Tenjin-cho, Kiryu-shi, Gunma 376-8515, Japan, and NMR Application Laboratory, Application & Research Center, Analytical Instruments Division, JEOL Ltd., 3-1-2, Musashino, Akishima-shi, Tokyo 196-0021, Japan

Received January 7, 1998; Revised Manuscript Received July 30, 1998

ABSTRACT: The relationship between the amide proton chemical shift and the conformation of homopolypeptides in the solid state was studied using the ^{1}H combined rotation and multiple pulse spectroscopy (CRAMPS) NMR method. The main-chain amide proton signals are considerably broad due to the residual dipolar couplings between the quadrupolar ^{14}N nucleus and amide proton relative to other proton signals of solid polypeptides. We have prepared fully ^{15}N-labeled (99 at. %) poly(L-alanines) ([Ala*]$_n$) and poly(L-leucines) ([Leu*]$_n$), adopting an α-helix or β-sheet form to eliminate the effect of the quadrupolar ^{14}N nuclei, and then measured their ^{1}H CRAMPS NMR spectra by increasing the magic-angle spinning speed. Thus, the ^{15}NH proton chemical shifts of [Ala*]$_n$ and [Leu*]$_n$ were successfully determined to be 8.0−8.1 ppm (α-helix) and 8.6−9.1 ppm (β-sheet). Accordingly, it became apparent that the amide proton chemical shifts are sensitive to the conformation of solid polypeptides.

Introduction

High-resolution and solid-state NMR spectroscopies, especially for the ^{1}H, ^{13}C, and ^{15}N nuclei, are very useful in the structural analysis of polypeptides and proteins in the solid state.[1−12] In our previous papers,[5,6,8−12] it has been demonstrated that the ^{15}N chemical shifts of amide nitrogens in solid polypeptides are related to the main-chain conformation, the neighboring amino acid sequence, and the nature of side chains of the individual amino acid residues, whereas the ^{13}C chemical shift of main-chain carbonyl carbons mainly depends on the conformation. Furthermore, we have very recently found that the ^{1}H chemical shift of the H_α signal from the methine protons, which was determined successfully by the ^{1}H CRAMPS (combined rotation and multiple pulse spectroscopy) method,[1] is very useful for conformational analysis of polypeptides in the solid state.

The ^{1}H CRAMPS method[13−19] has many advantages in comparison with the ^{13}C (and ^{15}N) CP-MAS (cross polarization−magic angle spinning) NMR methods: (1) it requires much smaller amounts of sample (10−15 mg or $^1/_{10}$th of that of the ^{13}C NMR measurement), (2) the measurement time may be about $^1/_{50}$th (only 5 min) of that of the ^{13}C NMR, and (3) the essential information on ^{1}H nucleus can be obtained. However, the ^{1}H CRAMPS method has simultaneously some disadvantages such as problems of line width broadening[14] and an unreliable chemical shift scale.[15−17] The latter has been now resolved by careful probe tuning and correction of drift using an internal standard, and therefore the ^{1}H chemical shift can be determined within an error limit of ±0.1 ppm in the important region (0−15 ppm) for organic compounds.[1] In our previous paper,[1] it has been found that (1) the H_α (methine proton) chemical shift of solid polypeptides is conformation-dependent: e.g., right-handed α-helix (α-helix) (3.9−4.0 ppm) and antiparallel β-sheet (β-sheet) forms (5.1−5.5 ppm), (2) the H_β (methyl proton) is strongly affected by the chemical structure of the individual amino acid residue, but it is almost insensitive to the main-chain conformation, and (3) the amide (NH) proton signal is very broad and unclear.

Although the fact that the conformation of solid polypeptides can be determined by the ^{1}H chemical shift was an important discovery, the problem of the very broad NH signal (which theoretically contains essential information about hydrogen bonding) was still unsolved. The amide proton signal broadening is due to the residual dipolar couplings between the quadrupolar ^{14}N nuclei and the amide protons. The ^{1}H−^{14}N dipolar couplings cause an asymmetric doublet pattern that highly disturbs the determination of the true amide proton chemical shift value in the ^{1}H NMR spectra.[20] Such a dipolar broadening is never observed in solution NMR because the dipolar coupling is averaged out by rapid molecular motion.

In this paper, therefore, two approaches have been performed to get a sharp amide proton signal. First, we have used the fully ^{15}N-labeled (99 at. %) polypeptides such as poly(L-alanine) ([Ala*]$_n$) and poly(L-leucine) ([Leu*]$_n$), to eliminate the effects of the quadrupolar ^{14}N nuclei. Second, we have measured their ^{1}H CRAMPS NMR spectra at two distinct spinning speeds (2.0 and 3.5 kHz), to reduce the magnitude of the dipolar broadening between the ^{15}N nuclei and the amide protons.

Using these techniques, we have been able to determine exactly the amide proton chemical shifts of solid polypeptides adopting the α-helix and β-sheet forms for [Ala*]$_n$ and [Leu*]$_n$. We now report these values and discuss the correlation between the amide proton chemi-

* Corresponding author. Tel & Fax: (+81)-277-301443. E-mail: shoji@bce.gunma-u.ac.jp.
† Gunma University.
‡ JEOL Ltd.

10.1021/ma980020+ CCC: $15.00
Published on Web 10/02/1998

Table 1. Synthetic Conditions, Conformational Characteristics, and ^{1}H Chemical Shifts of Homopolypeptides

			^{1}H chemical shift, δ (ppm)			
sample[a]	A/I[b]	conformation[c]	H_β[d] ($+H_\gamma$[d])	H_δ[d]	H_α[e]	NH[f]
H-[Ala]$_5$-NHBu		β-sheet	1.2		5.0	
[Ala]$_n$-5	(65)	α-helix	1.4		3.9	
[Ala*]$_n$-1	4	β-sheet	1.2		5.2	8.6
[Ala*]$_n$-2	100	α-helix	1.4		4.0	8.0
[Leu]$_n$-1	5	β-sheet[g]	0.9	1.5	5.5	
[Leu]$_n$-2	100	α-helix	0.8	1.7	4.0	
[Leu*]$_n$-1	5	β-sheet (+ α-helix)	0.9	1.6	5.4 (4.0)	9.1 (8.2)
[Leu*]$_n$-2	100	α-helix	0.8	1.6	4.0	8.1

[a] Abbreviations: Ala, L-alanine; Ala*, ^{15}N-labeled L-alanine; Leu, L-leucine; Leu*, ^{15}N-labeled L-leucine; NHBu, *n*-butylamide; α-helix, right-handed α-helix; β-sheet, antiparallel β-sheet. [b] The molar ratio of the monomer (A) to the initiator (I), which corresponds to the theoretical number-averaged degree of polymerization. [c] Conformations of the samples determined by the ^{13}C and ^{15}N CP-MAS NMR, IR, and far-IR spectroscopic methods. [d] Side-chain protons (H_β, H_γ, and H_δ). [e] α-Methine proton. [f] Amide proton measured using the MREV-8 pulse sequence at 3.5 kHz MAS speed. [g] Containing a small amount of α-helix.

cal shifts and the conformation (including hydrogen bonding) of polypeptides in the solid state.

Experimental Section

Materials. The L-alanine pentapeptide *n*-butylamide, H-[Ala]$_5$-NHBu, was synthesized by the activated ester method[21,22] and other polypeptide samples of natural abundance, [Ala]$_n$-5, [Leu]$_n$-1, and [Leu]$_n$-2, were synthesized by the *N*-carboxy α-amino acid anhydride (NCA) method[23,24] in our laboratory. The fully ^{15}N-labeled homopolypeptides such as [Ala*]$_n$ (99 at. % of ^{15}N purity; MASSTRACE, Inc.) and [Leu*]$_n$ (99 at. % of ^{15}N purity; MASSTRACE, Inc.), which show characteristic differences in conformation such as the α-helix and β-sheet forms, were prepared by the heterogeneous polymerization of the corresponding NCAs in acetonitrile with *n*-butylamine as an initiator.[23,24] Conformational characterization of these samples was made on the basis of the conformation-dependent ^{13}C and ^{15}N chemical shifts determined from the CP-MAS NMR methods,[5,6,8−11] and from the characteristic bands in the IR and far-IR spectra.[25,26] Synthetic conditions and conformational characteristics of these samples are summarized in Table 1, together with the ^{1}H chemical shift data.

^{1}H CRAMPS NMR Measurements. The solid-state ^{1}H CRAMPS NMR measurements were performed on a Chemagnetics CMX 300 spectrometer operating at 300 MHz, equipped with a 5 mm CRAMPS probe. Silicon-rubber (δ 0.12) relative to tetramethylsilane $(CH_3)_4Si$ (δ 0) was used as an internal standard. The ^{1}H CRAMPS NMR spectra were recorded first without an internal standard and then calibrated afterward with an internal silicon-rubber. Thus, experimental errors of the ^{1}H chemical shifts are estimated to be less than ±0.1 ppm (0−15 ppm). The BR-24 and MREV-8 pulse sequences[27,28] were used. The radio frequency (RF) powers and windows of duration (τ) of these pulse sequences were adjusted so as to obtain the best resolution for adipic acid.

BR-24 Pulse Sequence. The 90° pulse width was 1.3 μs for the BR-24 pulse sequence. The cycle time of the BR-24 was 108 μs, corresponding to a τ of 3 μs. The rotational frequency of MAS was controlled at 2.0 kHz. The ^{1}H chemical shift was calculated with the scaling factor 0.40 for all samples, which was determined experimentally.

MREV-8 Pulse Sequence. The 90° pulse width was 1.1 μs for the MREV-8. The cycle time of MREV-8 was 28.8 μs, corresponding to a τ of 2.4 μs. The rotational frequency was controlled at 3.5 kHz. The ^{1}H chemical shift was calculated with the scaling factor 0.53 for all samples, which was determined experimentally. The carrier frequency was selected carefully in order to avoid carrier noise overlapping with the peaks from samples. Under these conditions, the resolution of adipic acid was retained up to 3.5 kHz of rotational frequency.

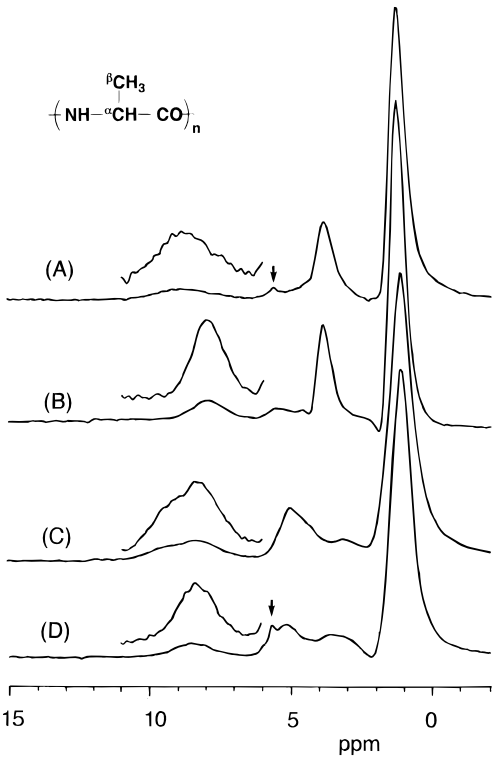

Figure 1. 300 MHz ^{1}H CRAMPS NMR spectra of α-helical and β-sheet poly(L-alanines) using the BR-24 pulse sequence at 2.0 kHz MAS speed: (A) [Ala]$_n$-5 (average degree of polymerization (DPn) = 65; natural abundance of ^{15}N; α-helix); (B) fully ^{15}N-labeled [Ala*]$_n$-2 (molar ratio of the monomer to initiator (A/I) = 100; 99 at. % purity of ^{15}N; α-helix); (C) H-[Ala]$_5$-NHBu (natural abundance of ^{15}N; β-sheet); (D) fully ^{15}N-labeled [Ala*]$_n$-1 (A/I = 4; 99 at. % purity of ^{15}N; β-sheet) in the solid state. Peak assignment: NH, 8.0−8.9 ppm; H_α, 3.9−5.2 ppm, H_β; 1.2−1.4 ppm. Note: $-N-CH_2-$ peak (3.2−3.5 ppm) of *n*-butylamide group in spectra C and D, and artifact (↓ sign) (5.7 ppm) in spectra A and D.

Results and Discussion

Observation of the ^{15}NH Proton Signal of ^{15}N-Labeled Poly(L-alanines). Figure 1 shows the 300 MHz ^{1}H CRAMPS NMR spectra of poly(L-alanines) in the α-helical and β-sheet forms using the BR-24 pulse sequence at 2.0 kHz MAS speed: (A) [Ala]$_n$-5 (natural abundance of ^{15}N, α-helix form), (B) [Ala*]$_n$-2 (99 at. % purity of ^{15}N, α-helix), (C) H-[Ala]$_5$-NHBu (natural abundance of ^{15}N, β-sheet), and (D) [Ala*]$_n$-1 (99 at. % purity of ^{15}N, β-sheet) in the solid state. The ^{1}H CRAMPS NMR spectra showed high-resolution proton signals separated into the three regions (NH, H_α, and H_β) for poly(L-alanines). The conformational characterization of [Ala]$_n$-5 (α-helix), [Ala*]$_n$-2 (α-helix), H-[Ala]$_5$-NHBu (β-sheet), and [Ala*]$_n$-1 (β-sheet form containing a small amount of α-helix) was confirmed by the H_α chemical shifts (α-helix, 3.9 ppm; β-sheet, 5.1 ppm),[1] which were in good agreement with the results obtained from the ^{13}C and ^{15}N CP-MAS NMR, IR, and far-IR spectra. The additional peaks around 3.2−3.5 ppm in spectra C and D and the small peak at 5.7 ppm in

spectra A and D were assigned to the $-N-CH_2-$ peak of the *n*-butylamide (−NHBu) group and an artifact, respectively.

It is noteworthy that the line shape of the NH proton signal of $[Ala^*]_n$-2 (α-helix) and $[Ala^*]_n$-1 (*β*-sheet), in which the quadrupolar effect is absent, exhibits a normal symmetric singlet pattern. By contrast, the line shape of the ^{14}NH signal of $[Ala]_n$-5 (α-helix) and H-$[Ala]_5$-NHBu (*β*-sheet) exhibits different kinds of asymmetric doublet patterns, which are attributable to the quadrupolar effect. The ^{15}NH proton signal of $[Ala^*]_n$-2 was somewhat sharp compared to the ^{14}NH signal of $[Ala]_n$-5. The half-width of the ^{15}NH signal of the α-helical ^{15}N-labeled poly(L-alanine) ($[Ala^*]_n$-2: 1.3 ppm) is smaller than that of the ^{14}NH signal of the sample of natural abundance ($[Ala]_n$-5: 2.3 ppm), as Figure 1A,B shows. Thus, it is clear that the quadrupolar ^{14}N nuclei are responsible for the signal broadening, and the asymmetric line shape of the amide proton peak, aside from the ^{15}NH signal, is still broad relative to the H_α and H_β signals. From the ^{1}H CRAMPS NMR spectra of α-helical ^{15}N-labeled poly(L-alanine), the true ^{15}NH chemical shift (*δ* 8.0) was determined, whereas the ^{14}NH chemical shift of $[Ala]_n$-5 could not be determined because of the quadrupolar splitting. Thus, it was shown that the determination of the true amide proton chemical shift of α-helical poly(L-alanine) can be achieved by replacement of the quadrupolar ^{14}N nuclei by the ^{15}N nuclei.

Next, we have measured the poly(L-alanine) samples by adopting the *β*-sheet form, to determine the NH proton chemical shifts characteristic of the *β*-sheet conformation and to check the effect of conformation on the NH proton signal broadening and the line shape. As shown in Figure 1C,D, the half-widths of the NH proton signals of H-$[Ala]_5$-NHBu and $[Ala^*]_n$-1 were 2.4 and 1.5 ppm, respectively, which are similar to those of α-helical poly(L-alanines). The ^{14}NH line shape of H-$[Ala]_5$-NHBu exhibits a typical asymmetric doublet pattern, however, which is quite different from that of the α-helical poly(L-alanine). The true ^{15}NH chemical shift could not be determined from the normal singlet pattern of $[Ala^*]_n$-1 because of the low S/N ratio, and neither could the ^{14}NH chemical shift of H-$[Ala]_5$-NHBu be determined.

Thus, it was found that (1) the quadrupolar ^{14}N nuclei are responsible for the NH signal broadening and the asymmetric line shape, (2) the asymmetric line shape is different between the α-helix and *β*-sheet conformations, and (3) the true ^{15}NH proton chemical shift of α-helical $[Ala^*]_n$-2 was 8.0 ppm but that of $[Ala^*]_n$-1 was difficult to determine because of the low S/N ratio.

Observation of the ^{15}NH Proton Signal of ^{15}N-Labeled Poly(L-leucines). Figure 2 shows the 300 MHz ^{1}H CRAMPS NMR spectra of α-helical and *β*-sheet poly(L-leucines) using the BR-24 pulse sequence at 2.0 kHz MAS speed: (A) $[Leu]_n$-2 (natural abundance, α-helix), (B) $[Leu^*]_n$-2 (99 at. % ^{15}N, α-helix), (C) $[Leu]_n$-1 (natural abundance, *β*-sheet), and (D) $[Leu^*]_n$-1 (99 at. % ^{15}N, *β*-sheet + α-helix) in the solid state. The ^{1}H CRAMPS NMR spectra show high-resolution proton signals (NH, H_α, and side chain protons) of poly(L-leucines). The α-helical conformation of $[Leu]_n$-2 and $[Leu^*]_n$-2 and the *β*-sheet conformation of $[Leu]_n$-1 and $[Leu^*]_n$-1 can be confirmed independently by the H_α chemical shift values (α-helix, 4.0 ppm; *β*-sheet, 5.5 ppm).[1] The peaks around 4.0 ppm in spectra C and D

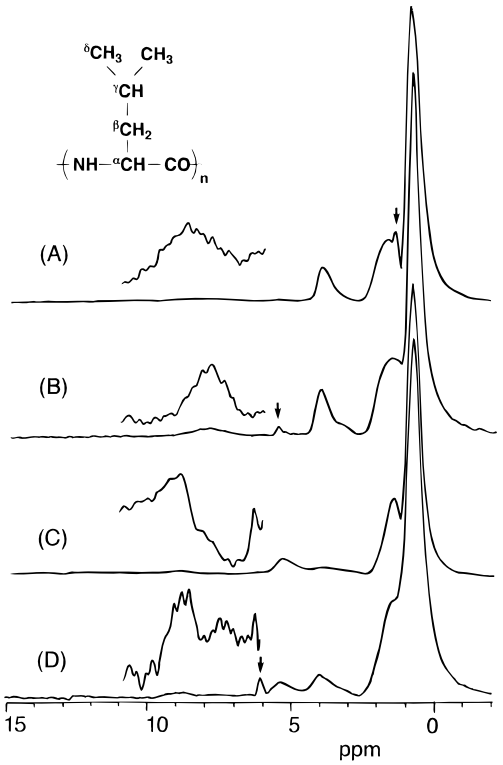

Figure 2. 300 MHz ^{1}H CRAMPS NMR spectra of α-helical and *β*-sheet poly(L-leucines) using the BR-24 pulse sequence at 2.0 kHz MAS speed: (A) $[Leu]_n$-2 (A/I = 100; natural abundance of ^{15}N; α-helix); (B) fully ^{15}N-labeled $[Leu^*]_n$-2 (A/I = 100; 99 at. % purity of ^{15}N; α-helix); (C) $[Leu]_n$-1 (A/I = 5; natural abundance of ^{15}N; *β*-sheet); (D) fully ^{15}N-labeled $[Leu^*]_n$-1 (A/I = 5; 99 at. % purity of ^{15}N; *β*-sheet + α-helix) in the solid state. Peak assignment: NH, 8.2−9.1 ppm; H_α, 4.0−5.5 ppm; H_β and H_γ, 0.8−0.9 ppm; H_δ, 1.5−1.7 ppm. Note: artifact (↓) (1.3 ppm in (A), 5.6 ppm in (B), and 6.1 ppm in (D)).

indicate that these samples contain the α-helix component, which was confirmed by the IR and ^{13}C CP/MAS measurements. Also, the small peak around 1.3 ppm in spectrum A, 5.6 ppm in spectrum B, or 6.1 ppm in spectrum D is an artifact.

The ^{15}NH proton signal of α-helical $[Leu^*]_n$-2 (B), in which the quadrupolar effect is absent, was somewhat sharper as compared to the ^{14}NH signal of the α-helical $[Leu]_n$-2 (A). The half-widths of the NH signal of $[Leu]_n$-2 and $[Leu^*]_n$-2 were 1.8 and 1.3 ppm, respectively, which are nearly the same as those of poly(L-alanines). However, the relative intensity of the ^{15}NH signal of $[Leu^*]_n$-2 is weaker than that of $[Ala^*]_n$-2, which is related to the ratio of the number of the amide proton to the side chain protons. The line shape of the ^{15}NH signal of $[Leu^*]_n$-2 exhibits an isotropic singlet pattern, whereas that of the ^{14}NH signal of $[Leu]_n$-2 is broad and unclear (probably an asymmetric doublet), as shown in Figure 2A. Thus the true ^{15}NH chemical shift of $[Leu^*]_n$-2 could not be determined from the spectrum because of the low S/N ratio, and neither could the ^{14}NH chemical shift of $[Leu]_n$-2.

Next, we discuss the *β*-sheet poly(L-leucine). The half-widths of the NH signals for *β*-sheet poly(L-leucines) could not be determined. The two ^{15}NH signals of $[Leu^*]_n$-1 are assigned to the *β*-sheet and α-helix forms. It was impossible to determine the true ^{15}NH chemical shift due to the very poor signal resolution. Thus, it may be concluded that (1) the quadrupolar ^{14}N nuclei

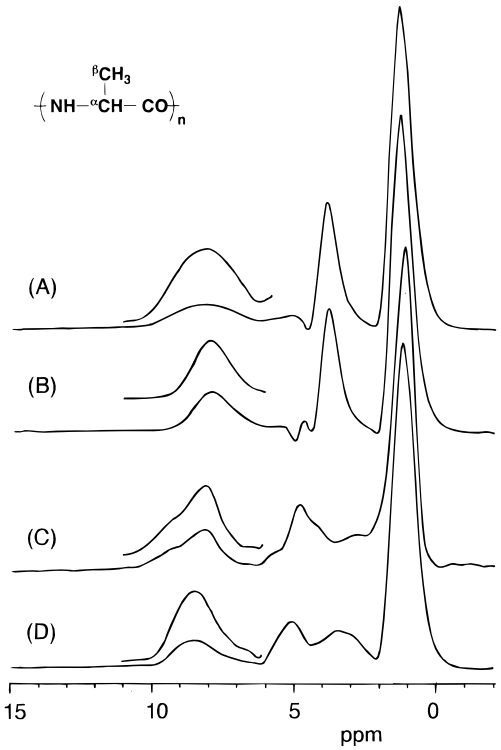

Figure 3. 300 MHz ^{1}H CRAMPS NMR spectra of α-helical and *β*-sheet poly(L-alanines) using the MREV-8 pulse sequence at 3.5 kHz MAS speed: (A) $[Ala]_n$-5 (α-helix); (B) ^{15}N-labeled $[Ala^*]_n$-2 (α-helix); (C) H-$[Ala]_5$−NHBu (*β*-sheet); (D) ^{15}N-labeled $[Ala^*]_n$-1 (*β*-sheet) in the solid state. Peak assignment: NH, 8.6 ppm (*β*-sheet) and 8.0 ppm (α-helix); H_α, 5.0−5.2 ppm (*β*-sheet) and 3.9−4.2 ppm (α-helix); H_β, 1.2 ppm (*β*-sheet) and 1.4 ppm (α-helix). Note: The additional peaks around 4.0−5.0 ppm in spectra A and B were assigned to career noise.

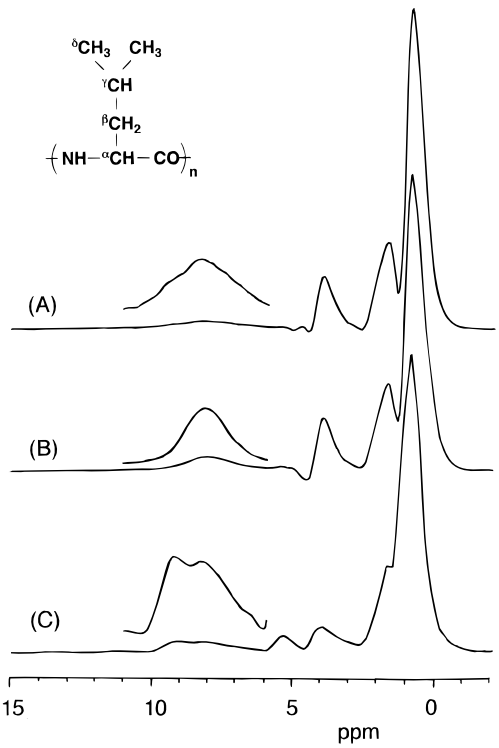

Figure 4. 300 MHz ^{1}H CRAMPS NMR spectra of α-helical and *β*-sheet poly(L-leucines) using the MREV-8 pulse sequence at 3.5 kHz MAS speed: (A) $[Leu]_n$-2 (α-helix); (B) ^{15}N-labeled $[Leu^*]_n$-2 (α-helix); (C) ^{15}N-labeled $[Leu^*]_n$-1 (*β*-sheet + α-helix) in the solid state. Peak assignment: NH, 9.1 ppm (*β*-sheet) and 8.1−8.2 ppm (α-helix); H_α, 5.4 ppm (*β*-sheet) and 4.0 ppm (α-helix); H_β and H_γ, 0.8−0.9 ppm; H_δ, 1.5−1.7 ppm. The additional peaks around 4.0−5.0 ppm in spectra A and B were assigned to career noise.

clearly contribute to the NH signal broadening and the asymmetric line shape, (2) the true ^{15}NH chemical shifts of poly(L-leucines) could not be determined because of the very low S/N ratio. The main cause of the ^{15}NH proton signal broadening for the fully ^{15}N-labeled polypeptides is due to the ^{15}N−^{1}H dipolar interaction, which will be discussed in the next section.

MAS Speed Dependency on the Amide Proton Signal Broadening. If the ^{15}N−^{1}H heteronuclear dipole interaction is the main reason for the ^{15}NH signal broadening, it is possible to obtain sharper NH peaks by faster MAS measurement. To confirm the dipolar interaction as the major contribution to signal broadening, we have measured the ^{1}H CRAMPS NMR of the fully ^{15}N-labeled polypeptides by increasing MAS speed. The best spectral resolution has been empirically obtained for the BR-24 pulse sequence[14] (MAS frequency of 1.5−2.0 kHz). However, this frequency is too slow to obtain sharper NH signals. A different pulse sequence is needed to allow the raising of the MAS frequency to more than 2.0 kHz, because both averaging techniques (MAS and multipulse averaging) interfere with each other and lead to a degradation in resolution.[29] Therefore, we have measured the 300 MHz ^{1}H CRAMPS NMR spectra of the fully ^{15}N-labeled polypeptides using the MREV-8 pulse sequence under the faster MAS speed of 3.5 kHz, which gave the best spectral resolution. It is known that the ^{1}H CRAMPS spectra above 4.0 kHz with the MREV-8 pulse sequence give spectra with poorer resolution than spectra at 3.5 kHz.

Figure 3 shows the 300 MHz ^{1}H CRAMPS NMR spectra of poly(L-alanines) in the α-helical and *β*-sheet forms using the MREV-8 pulse sequence at 3.5 kHz MAS speed: (A) $[Ala]_n$-5, (B) $[Ala^*]_n$-2, (C) H-$[Ala]_5$-NHBu, and (D) $[Ala^*]_n$-1 in the solid state. The additional peaks around 4.0−5.0 ppm in spectra A and B were assigned to career noise.

The intensity of the NH proton signals of poly(L-alanine) were increased by measuring with the MREV-8 pulse sequence at faster MAS speed (3.5 kHz). From the ^{1}H CRAMPS NMR spectra, therefore, we could successfully determine the ^{15}NH chemical shift value for $[Ala^*]_n$-2 (α-helix, *δ* 8.0), which is identical to the values determined with BR-24 (2.0 kHz). Further, we could determine the ^{15}NH chemical shift for $[Ala^*]_n$-1 (*β*-sheet, *δ* 8.6) using the MREV-8 pulse sequence at 3.5 kHz MAS speed. In contrast, the ^{14}NH chemical shift values for $[Ala]_n$-2 and $[Ala]_n$-1 were not determined because the line shapes of the ^{14}NH signals exhibit an asymmetric doublet pattern. Thus, it was found that the determination of the true NH chemical shift of poly(L-alanines) can be achieved to measure the fully ^{15}N-labeled samples under faster MAS speed (3.5 kHz) and that these chemical shifts depend on conformation (α-helix, *δ* 8.0; *β*-sheet, *δ* 8.6). This is the first determination of the true NH proton chemical shifts of poly(L-alanines) by the ^{1}H CRAMPS NMR.

Figure 4 shows the 300 MHz ^{1}H CRAMPS NMR spectra of poly(L-leucines) in the α-helical and *β*-sheet forms using the MREV-8 pulse sequence at 3.5 kHz MAS speed: (A) $[Leu]_n$-2, (B) $[Leu^*]_n$-2, and (C) $[Leu^*]_n$-1 in the solid state. The additional peaks around 4.0−

5.0 ppm in spectra A and B were assigned to career noise.

The intensity of the NH proton signals of poly(L-leucines) were increased by measuring with the MREV-8 pulse sequence at faster MAS condition (3.5 kHz). From the ^{1}H CRAMPS NMR spectra, therefore, we could successfully determine the ^{15}NH chemical shift value for $[Leu^*]_n$-2 (α-helix, δ 8.1) and for $[Leu^*]_n$-1 (β-sheet, δ 9.1; α-helix, δ 8.2). However, the ^{14}NH chemical shift values for $[Leu]_n$-2 were not determined. Thus, it was found that the determination of the true NH chemical shift of poly(L-leucines) can be achieved by measuring of the fully ^{15}N-labeled samples under faster MAS condition (3.5 kHz), and that these chemical shifts depend on conformation (α-helix, δ 8.1−8.2; β-sheet, δ 9.1).

Therefore, it was concluded that the ^{1}H CRAMPS method, which combined the relatively fast MAS (3.5 kHz) with MREV-8 pulse spectroscopy is very useful for the determination of the ^{15}NH chemical shift of solid polypeptides.

Correlation between the Amide Proton Chemical Shift and Main-Chain Conformation. We could determine the NH proton chemical shifts of the fully ^{15}N-labeled polypeptides under relatively fast MAS conditions with the MREV-8 pulse sequence. The NH chemical shifts of the fully ^{15}N-labeled homopolypeptides determined with the MREV-8 pulse sequence under faster MAS conditions are summarized in Table 1. It was found that the true ^{15}NH chemical shifts of the fully ^{15}N-labeled polypeptides are conformation-dependent: $[Ala^*]_n$-2 (α-helix, 8.0 ppm); $[Leu^*]_n$-2 (α-helix, 8.1 ppm); $[Ala^*]_n$-1 (β-sheet, 8.6 ppm); $[Leu^*]_n$-1 (β-sheet, 9.1 ppm; α-helix, 8.2 ppm). Thus, the ^{15}NH chemical shifts of poly(L-alanines) and poly(L-leucines) adopting the α-helix form appear upfield by 0.6−1.0 ppm compared with those of the β-sheet ones, and it is now possible to distinguish the α-helix and β-sheet conformations readily from their ^{15}NH chemical shifts. The above NH chemical shift differences between the α-helix and β-sheet forms seem to be related to the hydrogen bond lengths other than their conformations. According to the X-ray diffraction studies of poly(L-alanines) by Arnott et al.,[30,31] the distance between the nitrogen and oxygen atoms is 2.83 and 2.87 Å for the β-sheet and α-helical forms, respectively. Accordingly, the ^{15}NH proton chemical shifts of $[Ala^*]_n$-1 (β-sheet: hydrogen bond distance 2.83 Å) appear downfield in comparison with that of $[Ala^*]_n$-2 (α-helix: hydrogen bond distance 2.87 Å), which is qualitatively acceptable.

Next, we compared our results of polypeptides in the solid state to solution state NMR measurements,[32−34] attention being given to the dependence of the amide proton chemical shifts on conformation. As a result, we found that (1) the amide proton chemical shifts of the α-helical polypeptides in the solid state (8.0−8.2 ppm from TMS) are identical with those in solution[32] (7.96−8.04 ppm from DSS) and (2) the amide proton chemical shifts of the β-sheet polypeptides in the solid state (8.6−9.1 ppm from TMS) are, on the contrary, 0.1−0.6 ppm downfield from those in solution[32] (8.44−8.52 ppm from DSS). These results are very similar to the H_α chemical shift displacements for poly(L-alanines) and poly(L-leucines):[1] (1) the H_α chemical shifts of α-helical polypeptides in the solid state (3.9−4.0 ppm from TMS) are identical with those in solution[32] (3.94−3.95 ppm from DSS), and (2) the H_α chemical shifts of β-sheet polypeptides in the solid state (5.1−5.5 ppm from TMS) are 0.4−0.8 ppm downfield from those in solution (4.70−4.71 ppm from DSS). This is a very interesting finding and the main reason of these chemical shift difference can be explained by a solvent effect in solution.

Conclusion

In this study, we have synthesized and measured the fully ^{15}N-labeled poly(L-alanines) (α-helix and β-sheet forms) and poly(L-leucines) (α-helix and β-sheet), to eliminate the ^{14}N quadrupole effect. As a result, we have first determined the ^{15}NH chemical shifts of the fully ^{15}N-labeled polypeptides in the solid state by ^{1}H CRAMPS NMR using the MREV-8 pulse sequence at 3.5 kHz MAS speed. The true NH chemical shifts of the fully ^{15}N-labeled polypeptides depend on the conformation and hydrogen bond lengths: α-helix (8.0−8.2 ppm) and β-sheet form (8.6−9.1 ppm). Accordingly, the ^{15}NH proton chemical shift is very useful for the studies on the conformation and hydrogen bonds of polypeptides in the solid state.

Acknowledgment. This work was supported in part by a Grant-in-Aid for Scientific Research (B) from the Ministry of Education, Science, Sports, and Culture of Japan.

References and Notes

(1) Shoji, A.; Kimura, H.; Ozaki, T.; Sugisawa, H.; Deguchi, K. *J. Am. Chem. Soc.* **1996**, *118*, 7604−7607.
(2) Taki, T.; Yamashita, S.; Satoh, M.; Shibata, A.; Yamashita, T.; Tabeta, R.; Saito, H. *Chem. Lett.* **1981**, 1803−1806.
(3) Kricheldorf, H. R.; Müller, D. *Macromolecules* **1983**, *16*, 615−623.
(4) Saito, H.; Ando, I. In *Annual Reports on NMR Spectroscopy*; Webb, G. A., Ed.; Academic Press: London, 1989; Vol. 22, pp 209−290.
(5) Saito, H.; Tabeta, R.; Shoji, A.; Ozaki, T.; Ando, I. *Macromolecules* **1983**, *16*, 1050−1057.
(6) Shoji, A.; Ozaki, T.; Saito, H.; Tabeta, R.; Ando, I. *Macromolecules* **1984**, *17*, 1472−1479.
(7) Förster, H. G.; Müller, D.; Kricheldorf, H. R. *Int. J. Biol. Makromol.* **1983**, *5*, 101−105.
(8) Shoji, A.; Ozaki, T.; Fujito, T.; Deguchi, K.; Ando, I. *Macromolecules* **1987**, *20*, 2441−2445.
(9) Shoji, A.; Ozaki, T.; Fujito, T.; Deguchi, K.; Ando, S.; Ando, I. *Macromolecules* **1989**, *22*, 2860−2863.
(10) Shoji, A.; Ozaki, T.; Fujito, T.; Deguchi, K.; Ando, S.; Ando, I. *J. Am. Chem. Soc.* **1990**, *112*, 4693−4697.
(11) Shoji, A.; Ando, S.; Kuroki, S,; Ando, I.; Webb, G. A. In *Annual Reports on NMR Spectroscopy*; Webb, G. A., Ed.; Academic Press: London, 1993; Vol. 24, pp 55−98.
(12) Shoji, A.; Ozaki, T.; Fujito, T.; Deguchi, K.; Ando, I.; Magoshi, J. *J. Mol. Struct.* **1998**, *441*, 251−266.
(13) Pembleton, R. G.; Ryan, L. M.; Gerstein, B. C. *Rev. Sci. Instrum.* **1977**, *48*, 1286−1289.
(14) Bronnimann, C. E.; Hawkins, B. L.; Zhang, M.; Maciel, G. E. *Anal. Chem.* **1988**, *60*, 1743−1750.
(15) Schmidt-Rohr, K.; Spiess, H. W. In *Multidimensional Solid-State NMR and Polymers*; Academic Press: San Diego, CA, 1994; pp 70−134.
(16) Gerstein, B. C.; Dybowski, C. R. In *Transient Techniques in NMR of Solids*; Academic Press: London, 1985; pp 164−226.
(17) Gerstein, B. C. CRAMPS. In *Encyclopedia of Nuclear Magnetic Resonance*; Grant, D. M., Harris, R. K., Eds.; John Wiley & Sons: Ltd.: Chichester, U.K., 1996; Vol. 3, pp 1501−1509.
(18) Maciel, G. E.; Bronnimann, C. E.; Hawkins, B. L. In *Advances in Magnetic Resonance*; Academic Press: New York, 1990; Vol. 14, pp 125−150.
(19) Harris, R. K.; Jackson, P.; Merwin, L. H.; Say, B. J.; Hägele, G. *J. Chem. Soc., Faraday Trans. 1* **1988**, *84* (11), 3649−3672.
(20) Naito, A.; Root, A.; McDowell, C. A. *J. Phys. Chem.* **1991**, *95*, 3578−3581.
(21) Ozaki, T.; Oya, M.; Itoh, K. *Polym. J.* **1981**, *13*, 225−239.
(22) Ozaki, T.; Shoji, A.; Furukawa, M. *Makromol. Chem.* **1982**, *183*, 771−780.

(23) Oya, M. *J. Synth. Org. Chem. Jpn.* **1971**, *29*, 731−732.
(24) Shoji, A.; Kawai, T. *Kobunshi Kagaku* **1971**, *28*, 805−809.
(25) Miyazawa, T. In *Poly-α-Amino Acids*; Fasman, G. D., Ed.; Marcel Dekker: New York, 1967; pp 69−103.
(26) Ito, K.; Katabuchi, H.; Shimanouchi, T. *Nature, New Biol.* **1972**, *239*, 42−43 and references therein.
(27) Burum, D. P.; Rhim, W. K. *J. Chem. Phys.* **1979**, *71*, 944−956.
(28) Rhim, W. K.; Elleman, D. D.; Vaughan, R. W. *J. Chem. Phys.* **1973**, *59*, 3740−3749.
(29) Hafner, S.; Spiess, H. W. *J. Magn. Reson.* **1996**, Series A *121*, 160−166.
(30) Arnott, S.; Wonacott, A. L. *J. Mol. Biol.* **1966**, *21*, 371−383.
(31) Arnott, S.; Dover: S. D.; Elliot, A. *J. Mol. Biol.* **1967**, *30*, 201−208.
(32) Wishart, D. S.; Sykes, B. D. In *Methods in Enzymology*; James, T. L., Oppenheimer, N. J., Eds.; Academic Press: San Diego, CA, 1994; Vol. 239, pp 363−392.
(33) Wishart, D. S.; Sykes, B. D.; Richards, F. M. *FEBS Lett.* **1991**, *293*, 72−80.
(34) Wishart, D. S.; Sykes, B. D.; Richards, F. M. *J. Mol. Biol.* **1991**, *222*, 311−333.

MA980020+